JOURNAL OF PHYSICAL ORGANIC CHEMISTRY
J. Phys. Org. Chem. 2007; **20:** 992–997
Published online 7 August 2007 in Wiley InterScience
(www.interscience.wiley.com) DOI: 10.1002/poc.1237

N-(3,5-Di-*tert*-butylsalicylidene)-4-iodobenzene, a peculiar case of a nonlinear optical photoswitch

Arnaud Spangenberg,[1] Michel Sliwa,[1†] Rémi Métivier,[1] Romain Dagnélie,[1] Arnaud Brosseau,[1] Keitaro Nakatani,[1]* Robert Pansu[1] and Isabelle Malfant[2]

[1]PPSM, Institut d'Alembert, ENS Cachan, CNRS, UniverSud, 61 avenue du Président Wilson, F-94230 CACHAN, France
[2]LCC, CNRS, 205 route de Narbonne, F-31077 TOULOUSE, France

Received 31 January 2007; revised 22 May 2007; accepted 25 May 2007

ABSTRACT: *N*-(3,5-Di-*tert*-butylsalicylidene)-4-iodobenzene (**1**) is photochromic in the solid state, owing to its ability to yield enol–keto tautomerism. Despite its centrosymmetric structure ($P2_1/c$), polycrystalline thin films of **1** show second harmonic generation (SHG). Moreover, this SHG can be reversibly switched by light. Investigations using confocal microscopy showed that a morphology change occurs when the fundamental beam of a Ti:sapphire (990 nm, 1.3 ps) is focused on the material, yielding an SHG-active solid. Copyright © 2007 John Wiley & Sons, Ltd.
Supplementary electronic material for this paper is available in Wiley InterScience at http://www.mrw.interscience.wiley.com/suppmat/0894-3230/suppmat/

KEYWORDS: photochromism; nonlinear optics; anil; second harmonic generation; molecular switch

INTRODUCTION

Recently, substantial research has been focused on compounds that show a light-induced, reversible change of color. Interest in this phenomenon, known as photochromism, is due to its potential applications in information storage, electronic display systems, or optical switching devices.[1]

For the first time in 1909, Senier *et al*.[2] observed the reversible coloration of *N*-salicylideneaniline derivatives in the solid state. Nowadays, this family of compounds (also called anils or Schiff bases) is widely known:[3] upon irradiation in the UV, the yellow crystals change to red color, which disappears when the crystals are left in the dark or irradiated with visible light. Anils are very intriguing molecules, since the presence or absence of distortion between the two aromatic rings can lead respectively to photochromism or thermochromism.[4] Both phenomena are based on the same intramolecular enol–keto tautomerism, the former being photochemically and the latter thermally induced (Fig. 1). Strategies such as the substitution at aromatic rings by bulky groups (e.g., *tert*-butyl) favor photochromism, and also slow down the thermally induced back reaction from keto to enol.[5] Moreover, anils are also known for their good fatigue resistance during photoswitching.[6]

Among the properties that can be switched by photochromism, we have focused on second order nonlinear optical (NLO) properties,[7] and in particular on second harmonic generation (SHG). Switching these properties is of particular interest, since potential applications in telecommunications can be foreseen such as the development of switches or tuneable frequency converters.[8]

In the present paper, we report the synthesis and NLO properties of a new photochromic compound, *N*-(3,5-di-*tert*-butylsalicylidene)-4-iodobenzene (**1**) (Fig. 2). Although bearing neither strongly electron-donating nor -accepting groups, thin polycrystalline films of **1** exhibit efficient photo-induced SHG switching. In order to further understand the origin of the NLO properties of **1**, investigations were carried out by measuring SHG under a confocal microscope, and crystal structure of **1** was determined by X-ray diffraction. The results are compared with previous ones on the *N*-(3,5-di-*tert*-butylsalicylidene)-4-aminopyridine (**2**), an analogous compound which shows both photochromic and NLO properties (Fig. 2).[9]

EXPERIMENTAL

Synthesis and characterization

Reagents and solvents were used as received from Aldrich. Elemental analysis was performed by the Service

**Correspondence to:* K. Nakatani, PPSM, Institut d'Alembert, ENS Cachan, CNRS, UniverSud, 61 avenue du Président Wilson, F-94230 CACHAN, France.
E-mail: nakatani@ppsm.ens-cachan.fr
†Present Address: Katholieke Universiteit Leuven, Department of Chemistry, Institute for Nanoscale Physics and Chemistry (INPAC), Celestijnenlaan 200F, HEVERLEE, B-3001, Belgium.

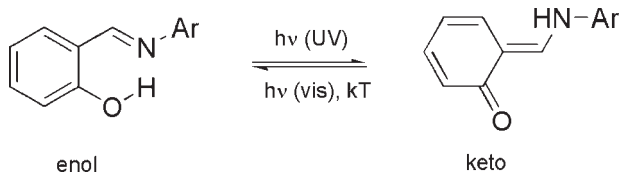

Figure 1. Tautomerism of anils. Ar can be a (substituted) phenyl, pyridine, or another aromatic ring

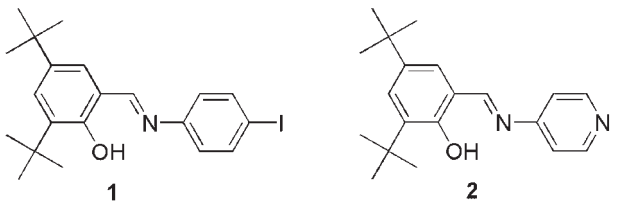

Figure 2. Formulae of *N*-(3,5-di-*tert*-butylsalicylidene)-4-iodobenzene (**1**) and *N*-(3,5-di-*tert*-butylsalicylidene)-4-aminopyridine (**2**)

de Microanalyse du CNRS (Gif sur Yvette and Vernaison). The ^{1}H NMR spectra were recorded on a Bruker AC 300 MHz spectrometer and FTIR spectra on a Thermo-Optek Nexus.

N-(3,5-Di-*tert*-butylsalicylidene)-4-iodobenzene (**1**) was synthesized by condensation of an equimolar amount of 3,5-di-*tert*-butyl-2-hydroxybenzaldehyde and 4-iodoaniline in a methanol solution containing a catalytic amount of paratoluenesulfonic acid. Yellow crystals were obtained after recrystallization in methanol with a 60% yield.

M.p. 160°C. Anal. Calcd for $C_{21}H_{26}INO$: C, 57.94%; H, 6.02%; N, 3.22%; I, 29.15%. Found: C, 57.86%; H, 6.18%; N, 3.21%; I, 28.95%.

^{1}H NMR (DMSO d^6, 300 MHz): $\delta = 1.27$ (s, 9H, tBu); 1.39 (s, 9H, tBu); 7.24 (dt, 2H, $J = 5.1$ Hz, Ar^{2}H); 7.39 (d, 1H, $J = 2.2$ Hz, Ar^{1}H); 7.48 (d, 1H, $J = 2.2$ Hz, Ar^{1}H); 7.78 (d, 2H, $J = 5.1$ Hz, Ar^{2}H); 8.96 (s, 1H, NCH); 13.70 (s, 1H, OH).

Ar^1 and Ar^2 correspond to aromatic enol and to aromatic aniline rings, respectively.

IR (cm^{-1}): 1616 (strong, C═N); 1601 (medium, aromatic); 1574 (strong, aromatic).

To compare the properties with the title compound, *N*-(3,5-di-*tert*-butylsalicylidene)-4-aminopyridine (**2**) samples were prepared. The detailed synthesis is described in Reference [9].

Sample preparation

Polycrystalline powder. Samples for powder test were made by putting recrystallized powder between two glass blades.

Single crystals. Recrystallization by slow evaporation of methanol yielded single crystals of **1**. Crystal size for X-ray diffraction was 0.3 mm × 0.3 mm × 0.2 mm.

Polycrystalline thin films. Polycrystalline thin films for spectroscopic and NLO measurements were prepared by melting the recrystallized powder between two glass blades. Average thickness was estimated to be around 14 and 23 μm respectively for **1** and **2**, from weight, area, and density based upon X-ray data.

Standard SHG measurements

Standard SHG measurements were made at the fundamental wavelength of 1907 nm (Nd:YAG nanosecond laser with a H_2 cell under 40 atm), similar to the Kurtz and Perry powder test.[10] SHG intensities of the solids were compared to that of urea powder.

SHG measurements under a confocal microscope

SHG was probed with a 990 nm fundamental laser beam (Ti:sapphire, 1.3 ps, 4 MHz). The beam was directed to the sample through the oil immersion objective (Olympus, 100×, NA = 1.3) of an inverted microscope using a dichroic mirror. The SHG was collected by the same objective, directed through a band-pass filter (350–650 nm) and focused via an optical fiber (Ø = 400 μm) onto a photomultiplier (Hamamatsu, Microchannel Plate R3809U-50). The optical fiber acts as a pinhole and gives an axial resolution a few micrometers. A CCD camera images simultaneously the sample. A XYZ piezo-stage allows the lateral and axial scanning by the laser beam. The intensity of the incident laser source was monitored by a photodiode.

Experiments under irradiation

The photochromic reaction was induced by an Hg/Xe lamp (Hamamatsu, LC6 Lightningcure, 150 W) equipped by filters of appropriate wavelengths. By irradiating the sample directly in the spectrophotometer (Varian Cary 5) or on the standard SHG test bench (see above), the photo-induced change of properties was measured *in situ*.

X-ray diffraction measurements

Data were collected at low temperature on an IPDS STOE diffractometer using a graphite-monochromated Mo-Kα radiation ($\lambda = 0.71073$ Å) and equipped with an Oxford Cryosystems Cryostream Cooler Device. The final unit cell parameters have been obtained by means of a

DOI: 10.1002/poc

least-squares refinement performed on a set of 2867 well measured reflections. The structures have been solved by Direct Methods using SIR92,[11a] and refined by means of least-squares procedures on a F^2 with the aid of the program SHELXL97[11b] included in the softwares package WinGX version 1.63.[11c] The Atomic Scattering Factors were taken from International Tables for X-ray Crystallography.[11d] All hydrogen atoms were calculated on a difference Fourier map and refined using a riding model. All non-hydrogen atoms were anisotropically refined.

Drawing of the molecule is performed with the program ORTEP32[11e] with 50% probability displacement ellipsoids for non-hydrogen atoms.

RESULTS AND DISCUSSION

Photochromic properties

The enol isomer of **1** exhibits absorption bands between 250 and 400 nm, both in the solid state and in solution. No color change was detected upon steady state UV irradiation in solution. This quite usual behavior of anils[12] is due to the fast thermal fading ($k = 1.7 \times 10^2\ s^{-1}$) of the red-colored keto species in solution. UV irradiation at 365 nm of a polycrystalline thin film evolved a strong absorption band in the visible area around 480 nm, typical of the keto form (Fig. 3). Under the conditions described in the experimental section, an absorption increase of 0.7 at 480 nm was observed. The back reaction can be induced by irradiation at 490 nm, or thermally by leaving the sample in the dark. This behavior can be compared to compound **2**. The kinetic data of the thermal reaction was analyzed by measuring the evolution of the absorbance at 480 nm after UV irradiation. The data were fitted by a double exponential. Although faster than for **2** (Table 2),[9] this thermal reaction is rather slow: $k_1 = 4.2 \times 10^{-5}\ s^{-1}$ and $k_2 = 4.8 \times 10^{-6}\ s^{-1}$. This result is in accordance with those of Kawato *et al.*[5b] on analogous compounds substituted by other halogen atoms, who found out that heavier substituents slow down the reaction. Alternate UV–visible irradiation cycles were performed several times without any noticeable irreversibility of the absorption changes.

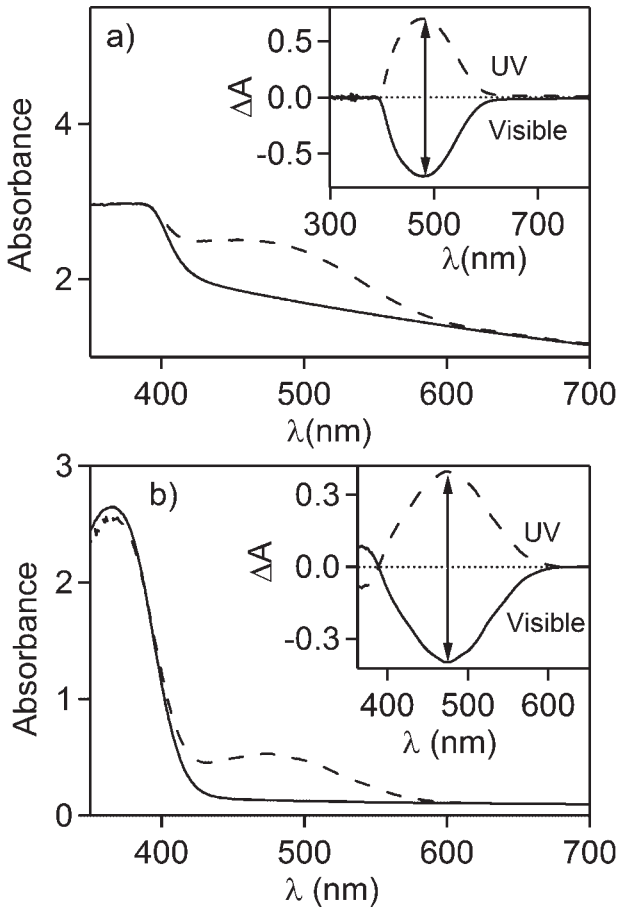

Figure 3. Transmission UV–visible absorption spectra of **1** (a) and **2** (b). Solid line: initial enol form, dashed line: mixture of enol and keto forms after irradiation at 365 nm. Inset shows the absorbance change with 365 nm (UV, enol to keto) and 490 nm irradiation (visible, keto to enol). Spectra of **2** were reproduced from Reference [9] with permission of the ACS

Table 1. Solid state SHG intensities for different types of samples

	1	**2**
Polycrystalline thin film	0.1–2	5–10
Polycrystalline powder	Ø[a]	3[b]
Single crystal	Ø[a]	Active[c]

Values are given *versus* urea.
[a] Ø means 'below detection limit'.
[b] From Reference [9].
[c] No appropriate reference single crystal is available.

Photo-induced switching of NLO properties

First, NLO properties of **1** were investigated at 1907 nm on a standard SHG test bench. As mentioned in Table 1, polycrystalline thin films gave an SHG signal, at most equal to 2 (*vs*. urea), but there was no detectable SHG from powder samples or from single crystals. In comparison the powder test of polycrystalline samples of **2** yielded an SHG intensity of 10 (*vs*. urea).

To test the ability of **1** to switch SHG upon light excitation, the SHG of a polycrystalline thin film was followed *in situ* during UV–visible irradiation cycles. The SHG change was reversible and reproducible at least for a few cycles, and the SHG contrast obtained under these conditions was *ca* 50% (Fig. 4). Although higher light-induced or electron-induced SHG contrasts were

DOI: 10.1002/poc

Table 2. Thermal back reaction rate constants at room temperature (298 K)

	k_1 (s^{-1})	k_2 (s^{-1})	Reference
F		1.6×10^{-2}	5b
Cl		1.0×10^{-3}	5b
Br	1.0×10^{-3}	1.8×10^{-4}	5b
I (**1**)	4.2×10^{-5}	4.8×10^{-6}	
2	3.6×10^{-5}	1.8×10^{-8}	9

F, Cl, Br, and I stand for *N*-(3,5-di-*tert*-butylsalicylidene)-4-fluorobenzene, -4-chlorobenzene, -4-bromobenzene, and -4-iodobenzene.

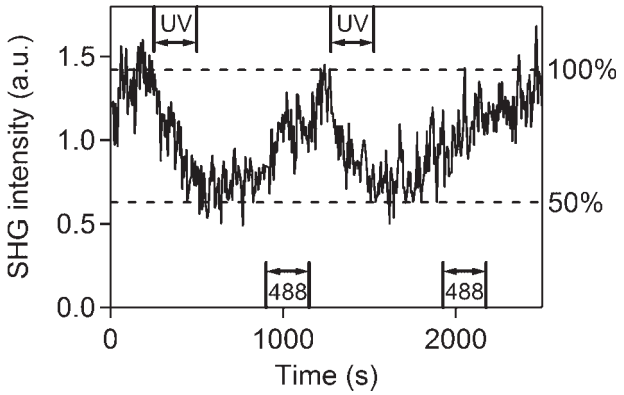

Figure 4. SHG photoswitching of a polycrystalline thin film of **1** under alternate UV (200–400 nm, 5 mW cm^{-2}) and visible (488 nm, 3 mW cm^{-2}) irradiations

reported in solution,[13] **1** exhibits the highest photo-induced SHG contrast yet reported in the solid state. For **2**, the contrast is 30% under similar conditions.[9]

Since both the fundamental and second harmonic beams were outside the absorption bands of both enol and keto isomers, the SHG change can be attributed to structural and/or NLO property changes of the material during the photo-induced reaction, rather than to the absorption change. The reason that SHG intensity decreases during the enol to keto reaction is due either to lower NLO properties of the latter isomer or to orientation changes.

Structure determination by X-ray diffraction

Since crystallographic structure is closely connected to SHG properties, and also to some extent to photochromic properties, structural determination of **1** was performed by X-ray diffraction.

The relationship between structure and SHG intensity has been extensively studied.[14] It is well established that a non-centrosymmetric structure is required to get an active SHG material. Hence, structural determination usually helps to rationalize solid state NLO properties. **2**

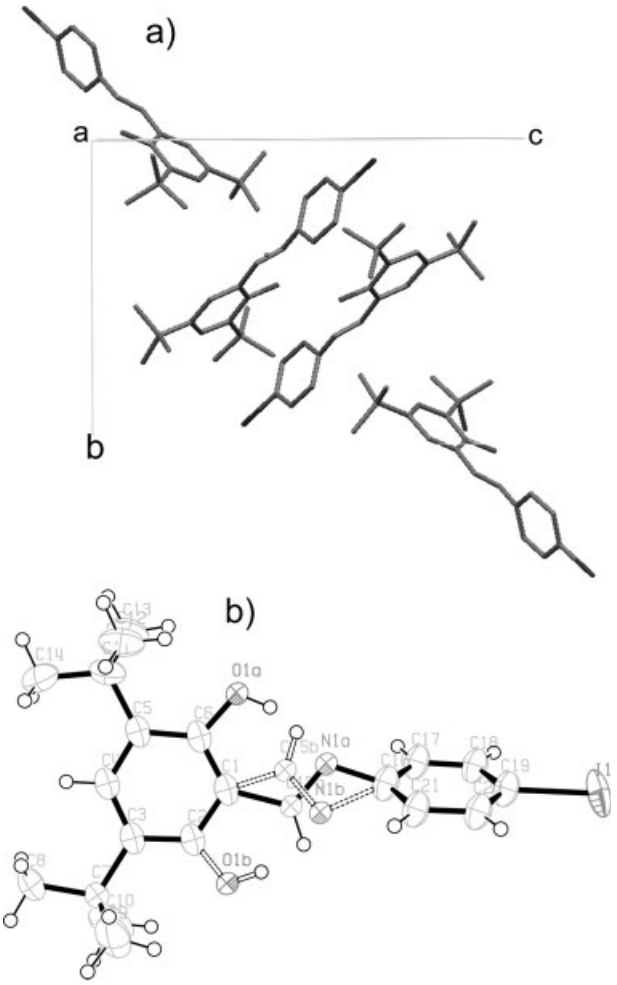

Figure 5. (a) Unit cell of **1**, view along the *a*-axis, showing a centrosymmetric structure. Hydrogen atoms are omitted. (b) ORTEP drawing of **1**, showing 50% probability displacement ellipsoids. The molecule is partially disordered on the C15 N1 O1 atoms with an occupancy factor of 0.64 (solid bonds)/0.36 (dotted bonds)

crystallizes in the non-centrosymmetric $P3_2$ space group, compatible with the presence of SHG properties.[9]

In the case of **1**, single crystal X-ray measurements gave a centrosymmetric monoclinic space group [$P2_1/c$, Fig. 5(a)]. The absence of detectable SHG from polycrystalline powder or single crystals is consistent with the centrosymmetry of the structure. The origin of the SHG in polycrystalline thin films of **1** is unusual, given the above-mentioned data. Hence further SHG measurements were performed, as described in the next section.

The structure of **1** is partially disordered on the C15 N1 O1 atoms with an occupancy factor of 0.64/0.36 [Fig. 5(b)]. As expected for photochromic anils,[3] **1** is not planar and the dihedral angle between the two 6-membered rings is 64.4° for the dominant structure. In thermochromic anils, this angle is close to 0°. This general feature of anils can be illustrated in other halogen-substituted anils: the 4-bromo-salicylidene-aniline, which

DOI: 10.1002/poc

is photochromic, has a dihedral angle of 42.8° between the two aromatic cycles,[15] and the 4-chloro-salicylideneaniline, which is thermochromic, has a dihedral angle of 5.9°.[16] The complete structural data of **1** is included as a Supplementary Material.

SHG measurements under a confocal microscope

In order to get a deeper insight on the SHG mechanism, behaviors of polycrystalline thin films of **1** and **2** were analyzed by confocal microscopy.[17]

The SHG intensity was followed during the *Z*-axis scan. At intensities below 2 MW cm^{-2}, **2** exhibits SHG, but **1** does not. The SHG scan of **2** gives a bell-shaped curve [Fig. 6(c)]. Although not perfectly symmetrical, its FWHM is 19 μm, which is close to the sample's thickness (23 μm). When the intensity is increased (>2 MW cm^{-2}), **1** becomes SHG active: the *Z*-axis scan shows two narrow peaks separated by a distance of 6 μm, which does not correspond to the initial sample thickness (14 μm). When the beam is immobilized on the sample, a persistent SHG signal can be recorded.

Figure 6a shows the initial image (area: 80 μm × 70 μm) of **1** recorded by a CCD camera. When the whole surface is irradiated by a high intensity laser beam (>2 MW cm^{-2}), the sample melts at the focal point, and solidifies with a new morphology when the beam is removed [Fig. 6(b)]. The new solid does not melt when the beam is focused on it. It is interesting to note that when the same procedure is applied to **2**, no such melting or morphology changes were observed. DSC measurements evidenced the existence of (at least) two crystalline and an amorphous states of **1**, and that heat cycles allow transformation between these forms (A. Spangenberg, A. Brosseau, R. Métivier, K. Nakatani, unpublished work). Due to this polymorphism, it is not surprising that the laser-induced melting–solidification process yields a new phase of material (apparently crystalline) that is SHG active, contrary to the initial form. Although experimental conditions differ, the same transformation probably induces SHG at 1907 nm (Fig. 4).

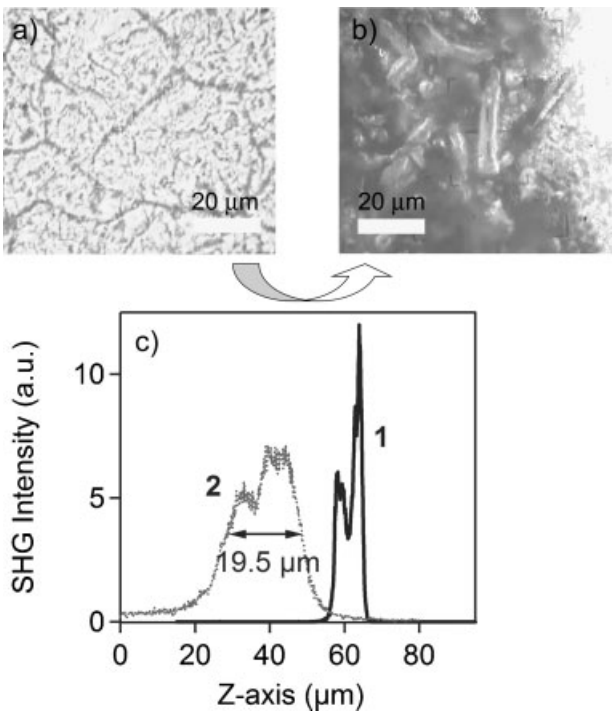

Figure 6. CCD camera pictures (area: 80 μm × 70 μm) of **1**: (a) initial form, and (b) newly formed solid after laser-induced melting (Ti:sapphire, 990 nm, >2 MW cm^{-2}). (c) SHG signal profile during *Z*-axis scan for **1** and **2** (for clarity, relative positions of the two samples have been displaced)

CONCLUSION

We have shown that **1** exhibits SHG signal as a polycrystalline thin film, even though its single crystal is centrosymmetric according to X-ray crystallography. Apparently an SHG-active form of **1** is locally generated by the fundamental laser beam. Combining this property with the photochromism, photoswitching of SHG can be performed efficiently. Some further fundamental experimental and theoretical investigations must be done in order to explain thoroughly the phase transition mechanism in **1** and the structure of its newly created SHG-active form. Also, as practical applications are concerned, repeatability of the SHG switching after several UV–visible irradiation cycles must be improved. The results presented in this paper encourage us to plan such investigations.

SUPPLEMENTARY MATERIAL

Structure of **1** is available free of charge at CCDC under the registration number 635611 (http://www.ccdc.cam.ac.uk).

Acknowledgements

The authors thank Mr Jean-Jacques Vachon for assistance on the laser set up. French Ministry of Research 'ACI Physico-Chimie de la Matière Complexe' program is acknowledged for funding.

REFERENCES

1. (a) *Chem. Rev.* 2000; 1683–1890; (b) *Molecular Switches*, Feringa BL (ed.). Wiley-VCH: Weinheim, 2003; 454.
2. (a) Senier A, Shepheard FG. *J. Chem. Soc.* 1909; **95**: 1943–1955; (b) Senier A, Shepheard FG, Clarke R. *J. Chem. Soc.* 1912; **101**: 1950–1958.

DOI: 10.1002/poc

3. (a) Hadjoudis E. In *Photochromism: Molecules and Systems*, Dürr H, Bouas-Laurent H (eds). Elsevier: Amsterdam, the Netherlands, 1990; 685–712; (b) Hadjoudis E, Mavridis IM. *Chem. Soc. Rev.* 2004; **33**: 579–588; (c) Amimoto K, Kawato T. *J. Photochem. Photobiol. C: Reviews* 2005; **6**: 207–226.
4. (a) Cohen MD, Schmidt GMJ, Flavian S. *J. Chem. Soc.* 1964; 2041–2051; (b) Fujiwara T, Harada J, Ogawa K. *J. Phys. Chem. B* 2004; **108**: 4035–4038.
5. (a) Kawato T, Koyama H, Kanatomi H, Isshiki M. *J. Photochem.* 1985; **28**: 103–110; (b) Kawato T, Koyama H, Kanatomi H, Tagawa H, Iga K. *J. Photochem. Photobiol. A: Chem.* 1994; **78**: 71–77.
6. Andes RV, Manikowski DM. *Appl. Opt.* 1968; **7**: 1179–1183.
7. Delaire JA, Nakatani K. *Chem. Rev.* 2000; **100**: 1817–1845.
8. (a) *Nonlinear optical properties of organic molecules and crystals*, vols **1** and **2**, Zyss J, Chemla DS (eds). Academic Press: Orlando, 1987; 482pp (vol. 1); 276pp (vol. 2); (b) *Nonlinear Optics of Organic Molecules and Polymers*, Nalwa HS, Miyata S (eds). CRC Press: Boca Raton, 1997; 884pp; (c) Zyss J. *C. R. Physique* 2002; **3**: 403–405.
9. Sliwa M, Létard S, Malfant I, Nierlich M, Lacroix PG, Asahi T, Masuhara H, Yu P, Nakatani K. *Chem. Mater.* 2005; **17**: 4727–4735.
10. Kurtz SK, Perry TT. *J. Appl. Phys.* 1968; **39**: 3798–3813.
11. (a) Altomare A, Cascarano G, Giacovazzo C, Guagliardi A. *J. Appl. Crystallogr.* 1993; **26**: 343–350; (b) SHELX97 [Includes SHELXS97, SHELXL97, CIFTAB]—Programs for Crystal Structure Analysis (Release 97-2). Sheldrick GM, Institüt für Anorganische Chemie der Universität, Tammanstrasse 4, D-3400 Göttingen, Germany, 1998; (c) Farrugia JL. *J. Appl. Crystallogr.* 1999; **32**: 837–838; (d) Cromer DT, Waber JT. In *International Tables for X-Ray Crystallography*, vol. **IV**, Kynoch Press: Birmingham, UK, 1974; Table 2.2B; 99pp. (e) Farrugia JL. *J. Appl. Crystallogr.* 1997; **30**: 565.
12. (a) Mitra S, Tamai N. *Phys. Chem. Chem. Phys.* 2003; **5**: 4647–4652; (b) Ziolek M, Kubicki J, Maciejewski A, Naskrecki R, Grabowska A. *Phys. Chem. Chem. Phys.* 2004; **6**: 4682–4689; (c) Ohshima A, Momotake A, Arai T. *J. Photochem. Photobiol. A: Chem.* 2004; **162**: 473–479.
13. (a) Coe BJ. *Chem. Eur. J.* 1999; **5**: 2464–2471; (b) Asselberghs I, Clays K, Persoons A, Ward MD, McCleverty J. *J. Mater. Chem.* 2004; **14**: 2831–2839.
14. Zyss J, Oudar JL. *Phys. Rev. A* 1982; **26**: 2028–2048.
15. Lindeman SV, Shklover VE, Struchkov YT, Kravcheny SG, Potapov VM. *Cryst. Struct. Comm.* 1982; **11**: 49–52.
16. Lindeman SV, Shklover VE, Struchkov YT, Kravcheny SG, Potapov VM. *Cryst. Struct. Comm.* 1982; **11**: 43–47.
17. Lagugné-Labarthet F, Shen YR. In *Advanced Methods in Contemporary Optical Systems and Microscopy*, volume 87 Series in Optical Sciences, Kao FJ, Torok P (eds). Springer: Berlin, 2003; 169–196.

DOI: 10.1002/poc